IOPscience iopscience.iop.org

Home Search Collections Journals About Contact us My IOPscience

Fabrication of dielectrophoretic microfluidic chips using a facile screen-printing technique for microparticle trapping

This content has been downloaded from IOPscience. Please scroll down to see the full text.

2015 J. Micromech. Microeng. 25 105015

(http://iopscience.iop.org/0960-1317/25/10/105015)

View the table of contents for this issue, or go to the journal homepage for more

Download details:

IP Address: 202.117.57.120
This content was downloaded on 29/10/2015 at 03:15

Please note that terms and conditions apply.

IOP Publishing Journal of Micromechanics and Microengineering
J. Micromech. Microeng. **25** (2015) 105015 (8pp) doi:10.1088/0960-1317/25/10/105015

Fabrication of dielectrophoretic microfluidic chips using a facile screen-printing technique for microparticle trapping

Wei Hong Wee[1,2,3], Zedong Li[2,3], Jie Hu[2,3], Nahrizul Adib Kadri[1], Feng Xu[2,3], Fei Li[2,4] and Belinda Pingguan-Murphy[1]

[1] Department of Biomedical Engineering, Faculty of Engineering, University of Malaya, Kuala Lumpur 50603, Malaysia
[2] Bioinspired Engineering and Biomechanics Center (BEBC), Xi'an Jiaotong University, Xi'an 710049, People's Republic of China
[3] The Key Laboratory of Biomedical Information Engineering of Ministry of Education, School of Life Science and Technology, Xi'an Jiaotong University, Xi'an 710049, People's Republic of China
[4] Department of Chemistry, School of Science, Xi'an Jiaotong University, Xi'an 710049, People's Republic of China

E-mail: feili@mail.xjtu.edu.cn and bpingguan@um.edu.my

Received 29 April 2015, revised 23 July 2015
Accepted for publication 28 July 2015
Published 15 September 2015

Abstract

Trapping of microparticles finds wide applications in numerous fields. Microfluidic chips based on a dielectrophoresis (DEP) technique hold several advantages for trapping microparticles, such as fast result processing, a small amount of sample required, high spatial resolution, and high accuracy of target selection. There is an unmet need to develop DEP microfluidic chips on different substrates for different applications in a low cost, facile, and rapid way. This study develops a new facile method based on a screen-printing technique for fabrication of electrodes of DEP chips on three types of substrates (i.e. polymethylmethacrylate (PMMA), poly(ethylene terephthalate) and A4 paper). The fabricated PMMA-based DEP microfluidic chip was selected as an example and successfully used to trap and align polystyrene microparticles in a suspension and cardiac fibroblasts in a cell culture solution. The developed electrode fabrication method is compatible with different kinds of DEP substrates, which could expand the future application field of DEP microfluidic chips, including new forms of point-of care diagnostics and trapping circulating tumor cells.

Keywords: dielectrophoresis (DEP), microfluidic chip, screen-printing technique, microparticle trapping and alignment

(Some figures may appear in colour only in the online journal)

1. Introduction

Trapping of microparticles (e.g. cells [1], bacteria [2], protozoa [3], polystyrene [4]) has found widespread applications in numerous fields, such as point-of-care diagnostics [5], high throughput screening [6], and drug analysis [7]. For instance, trapping of Malaria-infected red blood cells from a mixture consisting of healthy and infected cells is a very important step of preparation of blood samples for the clinical diagnosis of malaria [8]. For these applications, it is important to trap target microparticles on a testing platform to carry out detection tests with a high resolution and sensitivity. Microfluidic-based devices offer several advantages for microparticle trapping, including fast result processing, a small amount of sample required, high spatial resolution, user friendly operation, and low fabrication cost [9–11]. For example, a continuous-flow dielectrophoretic microfluidic device had been developed and applied to high throughput isolate and recover cancerous cells from blood samples [12].

Various microfluidic platforms have been developed for trapping microparticles based on different principles, such

 © 2015 IOP Publishing Ltd Printed in the UK

as dielectrophoresis (DEP) [13, 14], optical tweezers [15], acoustic waves [16], magnetophoresis [17], electrical means, and mechanical filtration etc [18]. Among these, DEP, which is concerned with the force experienced on a polarizable particle when subjected to non-uniform electric field, has attracted special attention due to its high accuracy of target selection [19], label free, simple instrumentation and scalability [20]. For instance, nanometer-sized beads and stem cells were trapped and separated from a mixture in a continuous-flow microfluidic system with a local dielectrophoretic force on multiple strip electrodes [21]. But the current DEP microfluidic devices are usually fabricated through expensive microfabrication techniques (e.g. thin-film deposition, sputtering, chemical vapor deposition [22]), which are complicated, time-consuming and not suitable for mass production [23]. Besides, a few types of materials, such as polymethyl-methacrylate (PMMA) [24], silicon, glass [25], poly(dimethylsiloxane) (PDMS) [26] and paper etc [27, 28], have been chosen as substrates of microfluidic chips to meet the demands of different applications [29, 30]. However, most existing fabrication methods are limited to certain substrate materials, rather than being adaptable. Further, disposable DEP microfluidic devices are preferred due to the potential issue of electrode damage and sample contamination as induced by the electrolyte electrolysis process on the electrode surface in the DEP procedure [31]. Therefore, it is important to develop a low cost, facile, and rapid method to fabricate disposable DEP microfluidic chips with different substrates for different applications.

The screen-printing technique is a common technique for fabrication of electrodes on various substrates with the advantages of fast processing, low fabrication cost, and high throughput [32], all of which make it suitable for DEP electrode fabrication. However, the application of screen-printing technique in DEP electrode fabrication has not yet been widely explored. In this paper, we developed a new facile method based on the screen-printing technique for fabrication of the electrodes of DEP chips on three types of substrates, including PMMA, poly(ethylene terephthalate) (PET) and A4 paper. And the fabricated PMMA-based DEP microfluidic chip, as an example, was successfully used to trap and align polystyrene (PS) microparticles in a suspension and cardiac fibroblasts in a cell culture solution. The developed electrode fabrication method is compatible with different types of DEP substrates, which could help to enhance the possibility of particle manipulation on aforementioned materials as microfluidic chip substrates and expand the application field of DEP microfluidic chips, such as in point-of care diagnostics and trapping circulating tumor cells, in the future.

2. Materials and methods

2.1. Theory of DEP

In a DEP experiment, the magnitude of particle displacement is proportional to the force exerted on the particle. The relationship between frequency and applied force is given by (equation (1)):

$$\boldsymbol{F_{DEP}} = 2\pi \mathbf{r}^3 \varepsilon_{\mathbf{m}}\, \mathbf{Re}[\boldsymbol{K}(\boldsymbol{f_{cm}})]\, \nabla \mathbf{E}^2 \tag{1}$$

where r is the radius of the particle, ε_m is the medium permittivity, ∇ is the Del operator (gradient) on the applied electric field E. Re$[K(f_{cm})]$ is the real part of the Clausius–Mossotti factor, which is given by (equation (2)).

$$\boldsymbol{K}(\boldsymbol{f_{cm}}) = \frac{\boldsymbol{\varepsilon_p^*} - \boldsymbol{\varepsilon_m^*}}{\boldsymbol{\varepsilon_p^*} + 2\boldsymbol{\varepsilon_m^*}} \tag{2}$$

where $\boldsymbol{\varepsilon_p^*}$ and $\boldsymbol{\varepsilon_m^*}$ are the complex permittivities of the particle and the medium, respectively, which can be further described by (equation (3)):

$$\boldsymbol{\varepsilon^*} = \boldsymbol{\varepsilon_0 \varepsilon} - \frac{\boldsymbol{j\sigma}}{\boldsymbol{\omega}} \tag{3}$$

where ε is the permittivity, ω is the angular frequency, j is the square root of -1 and σ is the conductivity of the particle. According to the above equations, in order to determine the permittivity and conductivity of the particle, derivation of the measurement of cell motion as a function of frequency can be used [33].

2.2. Fabrication of DEP microfluidic chips

As shown in figure 1, the DEP chip consists of two parts, i.e. a micro-channel covering an electrode chip. Taking a PMMA-based DEP microfluidic chip as an example, the fabrication process is described as follows.

A PMMA substrate (1 mm thickness), covered with a single slice of PET film (figure 1(a)), was cut out by a laser cutter (Versa LASER VLS3.50) to form an integrated electrode pattern with line width of ca. 300 μm and gap width of ca. 400 μm, which was designed by Corel Draw 12 software (figure 1(b)). Conductive silver (Ag) ink (C1002, Acheson, USA) was screen-printed on the electrode pattern of the PET film by a brush (figure 1(c)). The PMMA substrate with the printed Ag ink was placed into an oven at 120 °C for 30 min to cure the Ag ink. Then, the PMMA substrate integrated with the Ag electrodes after tearing off the PET thin film (figure 1(d)). The final DEP microfluidic chip was formed by covering the integrated PMMA substrate with another PMMA plate, which with a central channel with area about 20 mm^2, using a 120 μm-thickness double sided tape (figure 1(e)). The preparation procedures for the PET-based and the A4 paper-based DEP microfluidic chips are similar to the above procedure, except changing the substrates to PET or A4 paper, respectively.

2.3. Preparation of sample solutions

Two kinds of sample solutions were used in this work. One solution is the polystyrene bead suspension, which was prepared by diluting aqueous solutions with a specific size of PS beads (diameters of 3 μm, 5 μm or 10 μm,

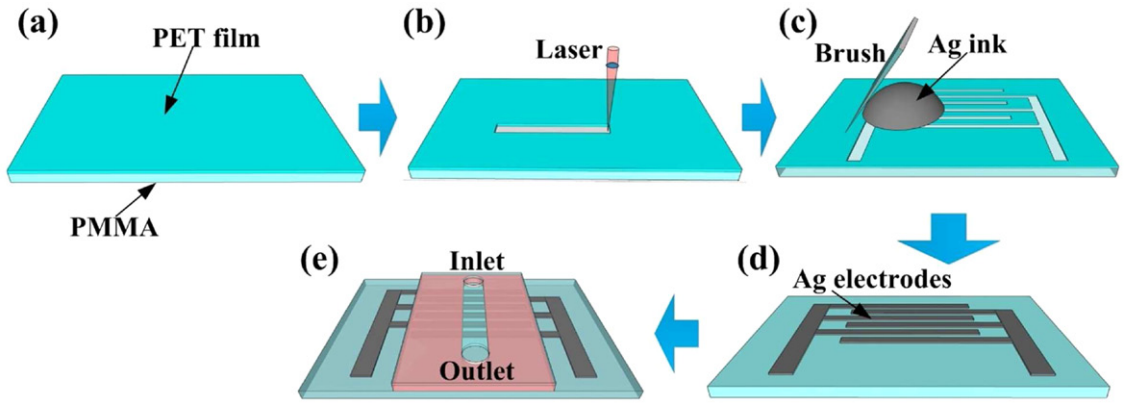

Figure 1. Scheme of the fabrication procedure of a DEP microfluidic chip on a PMMA substrate. (a) A PMMA substrate covered with a PET film on top. (b) A pattern for conductive ink printing was formed on the PMMA substrate by cutting the PET film using a laser cutter. (c) Conductive silver ink was screen-printed on the electrode pattern of the PET film by a brush. (d) The PMMA substrate integrated with the Ag electrodes was formed by curing Ag ink and tearing off the PET film. (e) The PMMA substrate integrated with the Ag electrode was covered by a PMMA plate with a microchannel on its top.

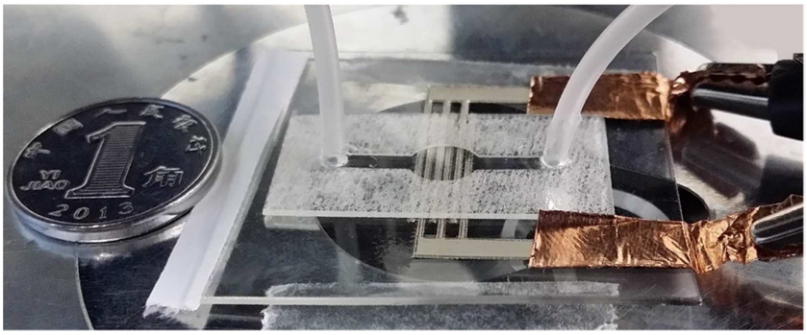

Figure 2. A photograph of the DEP experimental setup with a PMMA based DEP microfluidic chip placing on a microscope stage. A Chinese coin of 10 cent with diameter of 18 mm was placed besides the DEP chip for size comparison.

Aldrich-Sigma) with deionized (DI) water in volume ratios of 1:50 (6.77×10^{27} beads ml^{-1}), 1:40 (1.46×10^{27} beads ml^{-1}) and 1:20 (1.83×10^{26} beads ml^{-1}), respectively. The prepared three suspensions were ultrasonicated for 5 min to generate homogenous PS bead solutions. The other solution is the cardiac fibroblast solution, in which the cardiac fibroblasts were isolated from the heart of neonatal Sprague–Dawley rats (1–3 d-old) and the sample solution was prepared according to the following protocol. First, the heart tissues of rats were surgically removed following euthanasia. Then the heart tissues were washed with phosphate buffered saline (PBS) (pH = 7.4, Sigma-Aldrich) and minced into small pieces. Tissue digestion was performed using 0.8% collagenase type II enzyme (MP Biomedicals, Aurora, USA) solution at 37 °C with agitation. The pellets were resuspended in a cell culture medium composed of Dulbecco's Modified Eagle's medium (DMEM)/Ham F-12, 10% fetal bovine serum (FBS) and 1% antibiotic/antimycotic (Gibco, New York, USA), and then plated for 45 min in a cell culture dish at 37 °C and 5% CO_2. This allows preferential attachment of cardiac fibroblasts to the cell culture dish. Then, the cell culture medium containing cells (mainly cardiomyocytes) was removed and replaced with fresh cell culture medium [34]. The cardiac fibroblasts on day 2 after isolation were used for the DEP experiments, and the cell density of 10^6 cells ml^{-1} was calculated by a cell counting process using a Haemocytometer and Trypan blue solution.

2.4. DEP experimental setup and experimental procedure

The DEP experimental setup used in this work is shown in figure 2, in which a fabricated DEP microfluidic chip was placed and stabilized on the stage of an inverted microscope (Olympus IX 81, Japan) using a double sided tape. Two tubes were used to connect the inlet port of the DEP chip to a syringe pump and the outlet port of the DEP chip to a reservoir.

Before the DEP experiments, the sample solutions of PS beads or cardiac fibroblasts were injected into the microchannel of the DEP microfluidic chip through the input port using a hydrostatic pump with different flow rates (0.1–0.3 mL h^{-1}). During DEP experiments, an arbitrary waveform generator (ED1411, Zhongce Electronics, China) was employed to create the sinusoidal signals (20 V peak-to-peak (V_{pp}) ac voltage, frequency range of 1 kHz–10 MHz) and deliver these signals to the Ag electrodes of the DEP microfluidic chip. Copper conductive tapes were used to connect the Ag electrodes to the clamps of the waveform generator. The movements of the PS beads and the cardiac fibroblasts were observed under microscope using the objective lens at

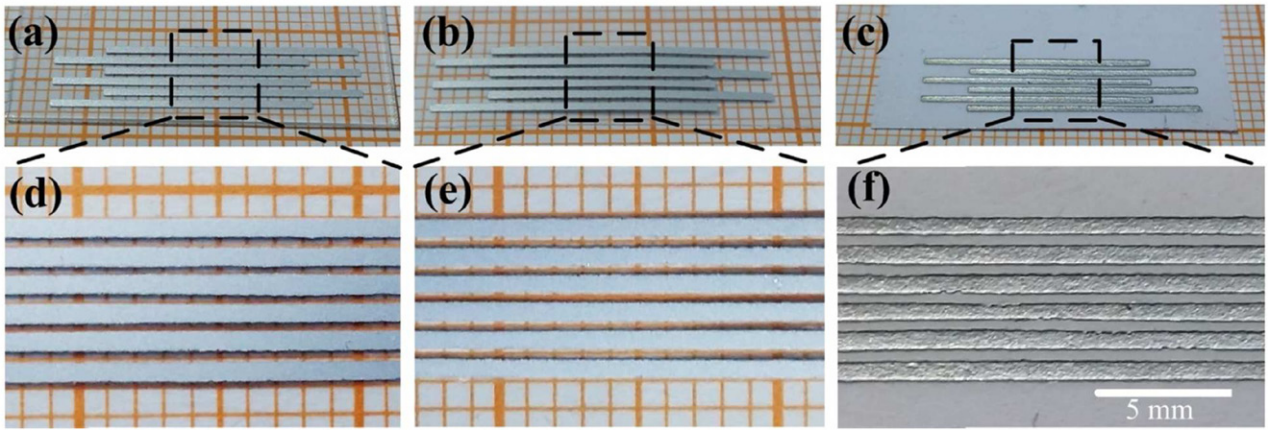

Figure 3. (a)–(c) Photographs and (d)–(f) microscopic images of the Ag electrode patterns printed on different substrates: (a), (d) a PMMA substrate, (b), (e) a PET substrate, and (c), (f) an A4 paper substrate. The background substrates are the graph papers with squares of 1 × 1 mm (length × width).

10 ×, 20 × and 40 × magnifications under bright field, and the images and videos were captured by a camera attached to the microscope. The values of various experimental parameters, such as microparticle size, biological cell type, applied frequency value, suspension medium and applied ac voltage, were carefully selected for the DEP experiments. To avoid the appearance of sudden electrolysis of electrolyte caused by the capacitive effect during DEP experiments, the magnitude and frequency of the ac signals were slowed down gradually during the switch-off process and the phrase changing stage. After each DEP experiment, the sample solution was transferred from the DEP microfluidic chip to a collecting tube.

3. Results and discussion

3.1. Screen-printed Ag electrode patterns on different substrates and their conductivity and surface uniformity

In this work, we selected the conductive silver ink as the DEP electrode material based on its liquid state under room temperature, and thus being suitable for screen printing. Using our method, Ag conductive inks were screen-printed on three representative substrate materials of microfluidic chips, i.e. PMMA, PET and paper, and the obtained DEP chips with Ag electrode patterns are shown in figures 3(a)–(c). In the figure, the Ag electrode patterns (with average width of 611 ± 17 μm and electrode gap width of 227 ± 34 μm) were uniformly formed on PMMA (figure 3(a)), PET (figure 3(b)) and A4 paper (figure 3(c)), respectively. It proves the feasibility of our screen-printing method for fabricating the electrode pattern of DEP chip on different substrates, which could contribute to the further combination of the DEP technique with the microfluidic chips with different substrates. However, compared to the designed electrode width (400 μm) and electrode gap (300 μm) on the PET mask mentioned above, the increase of the Ag electrode width and the decrease of the electrode gap might be due to the baking process of the Ag ink making the electrode size expand and then the gap squeeze. The surface uniformity and the conductivity of the fabricated Ag electrodes were also characterized. From the microscopic images of the Ag electrode lines on these substrates shown in figures 3(d)–(f), we observed that the Ag inks were well printed on these three substrates with uniform width and straight and obvious electrode boundary. The resistance of each fabricated Ag electrode was measured by a multimeter (UT58A, UNI-T, China) and found to be 15.02 ± 1.26 Ω cm^{-1}, 19.58 ± 5.13 Ω cm^{-1} and 16.92 ± 3.04 Ω cm^{-1}, respectively. Such good conductivities indicate the suitability of all substrates to be used as the electrodes of DEP microfluidic chips. Results were consistent among substrates, independent of hardness and translucency. However, compared to traditional DEP electrode fabrication techniques, such as electrochemical etching, metal deposition or photolithography, which could fabricate DEP electrodes from as small as a few hundred nanometers to less than 1 mm [35], the size and the surface homogeneity of the electrodes fabricated by our developed screen-printing method are still larger and coarser. Further improvement of the resolution of our method is needed in the future work.

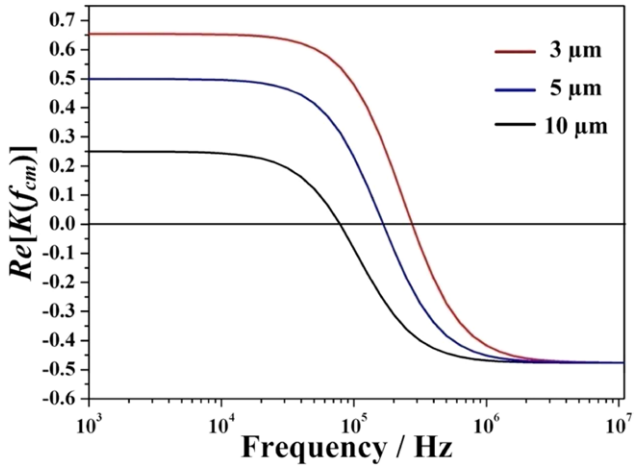

Figure 4. Relationship of Re[$K(f_{cm})$] versus Frequency for microparticles with diameters of 3 μm (red curve), 5 μm (blue curve) and 10 μm (black curve), respectively.

3.2. Effect of DEP on microparticle crossover frequency

We analyzed the DEP spectra with using PS beads as sample microparticles for the following particle trapping test. The

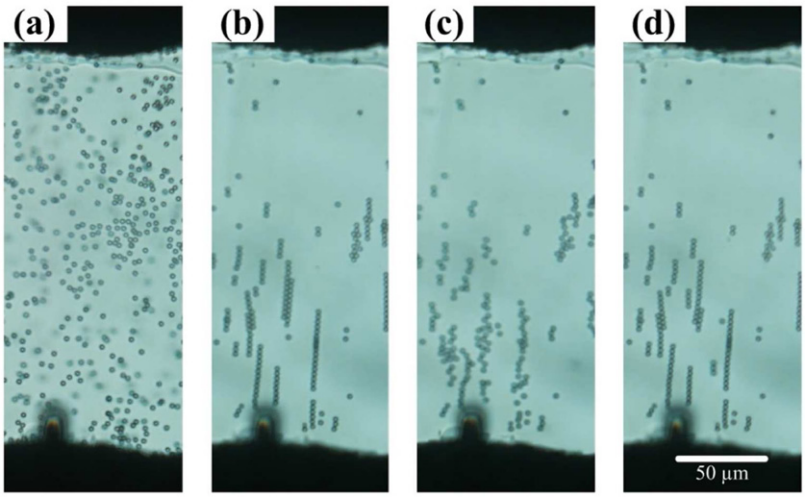

Figure 5. Microscopic images of a 3 μm-diameter PS beads suspension in the microchannel of a fabricated PMMA-based DEP microfluidic chip (magnification of 40×). (a) Before applying a sinusoidal signal to the DEP chip; (b) applying an ac voltage of 20 V_{pp} with frequency of 1 MHz to the two Ag electrodes of DEP chip for 5 min; (c) after switching off the applied signals; (d) re-applying the sinusoidal signals to the electrodes.

deionized water used had a measured conductivity value of 2.0×10^{-4} S m^{-1} and a relative permittivity of 78.5. The overall conductivity of PS beads is defined as $\sigma_{bulk} + \frac{2K_s}{r}$, where σ_{bulk} is the bulk conductivity (negligible for polystyrene particles), r is the average radius of PS beads, and K_s is the total surface conductance (composed of the contributions of the Stern layer and diffuse layer formed around the particles). According to the product information, the relative permittivity of the PS beads is 2.55. To check the function of the fabricated DEP microfluidic chip for microparticle trapping, the crossover frequencies (i.e. the change from positive DEP (p-DEP) to negative DEP (n-DEP)) of PS beads were measured by increasing the applied frequencies from lower values to higher ones. To reduce the probability of sudden electrolysis of electrolyte caused by the capacitive effect, the frequencies of ac signals were increased and decreased gradually during DEP experiments. At lower frequencies, the PS beads clearly exhibited a p-DEP effect and assembled to the positions close to the electrode. When the PS beads showed a n-DEP effect, they repelled from the electrode and assembled at the gap between electrodes. For the 3 μm-, 5 μm- and 10 μm-diameter PS beads, the crossover frequencies were 295 ± 30 kHz, 148 ± 12 kHz and 64 ± 7.1 kHz, respectively. Using the obtained crossover frequencies and equation (2), the overall conductivities of PS beads were calculated to be 1.6×10^{-3} S m^{-1}, 9.6×10^{-4} S m^{-1} and 4.8×10^{-4} S m^{-1} for the PS beads with diameters of 3 μm, 5 μm and 10 μm, respectively. Based on the above results, the relation between Re[$K(f_{cm})$] and frequency is illustrated in figure 4. Considering that the cardiac fibroblasts we used have an approximately spherical shape and a diameter about 10 μm (similar to the 10 μm-diameter PS beads), we did not calculate their crossover frequency again. Since the single-shell model was used for the DEP experiments for trapping cardiac fibroblasts, the obtained crossover frequency of 10 μm-diameter PS beads was also applied for the cardiac fibroblasts to achieve the objective of cell trapping [36].

3.3. Trapping of microparticles with different diameters using the fabricated DEP microfluidic chip

To test the performance of our fabricated DEP microfluidic chip for microparticle trapping, we selected a PMMA based DEP microfluidic chip and a suspension with 3 μm-diameter PS beads as the DEP chip and the first sample solution, respectively. The obtained DEP experimental results are shown in figure 5. Before applying the sinusoidal signal to the DEP chip, the PS beads were homogenously and randomly distributed in the microchannel of the DEP chip (figure 5(a)). When applying an ac voltage of 20 V_{pp} with a frequency of 1 MHz to the two Ag electrodes, the 3 μm-diameter PS beads started to move and were repelled under the DEP force, and finally arranged in a chain-shape along the gap between the two electrodes after 5 min (figure 5(b)), which indicates that the PS beads experienced a n-DEP force. The final trapping and alignment positions of these PS beads were close to the bottom electrode, which is due to the effect of the strength of the DEP force distribution leading to the alignment of PS beads at the positions of lower electrical field. After switching off the applied signals, the PS beads were released from the DEP force and spread away from the original chain (figure 5(c)). When applying the same sinusoidal signals as in figure 5(b) to the electrodes again, the PS beads were trapped and aligned at similar positions as the previous process (figure 5(d)), proving the repeatability of the fabricated DEP device for trapping the PS microparticles.

To further prove the capability of our fabricated DEP microfluidic chip to trap microparticles with bigger sizes and from mixed solution, a suspension with 5 μm- and 10 μm-diameter PS beads was used as the second sample solution. The same DEP experimental procedure was performed on the DEP microfluidic chip injected with the PS beads mixture and the obtained results are represented in figure 6.

As shown in figures 6(b) and (d), after applying an ac voltage of 20 V_{pp} with frequency 1 MHz to the electrodes,

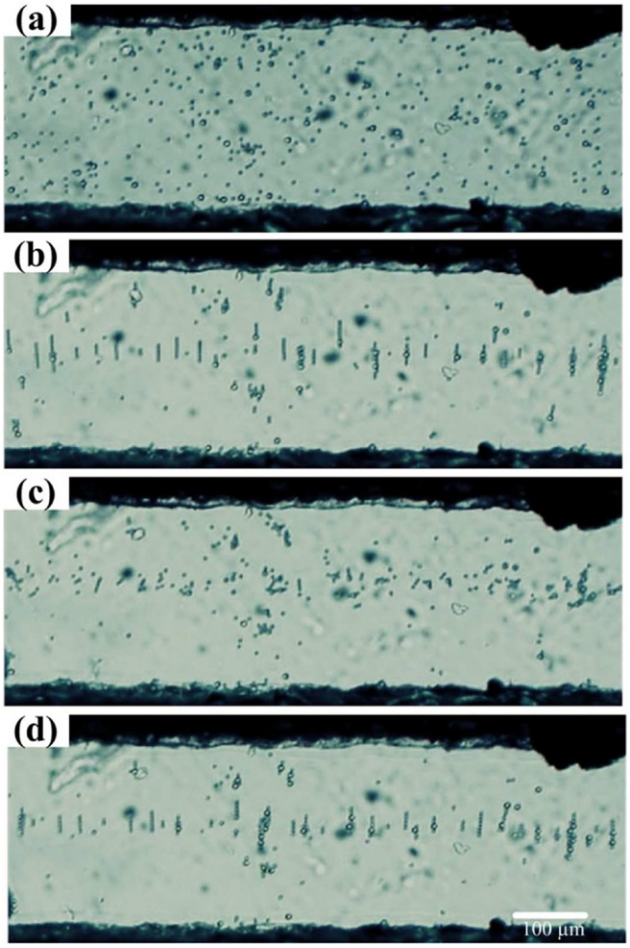

Figure 6. Microscopic images of a suspension with a 5 μm- and 10 μm-diameter PS beads mixture in the microchannel of a fabricated PMMA-based DEP microfluidic chip (magnification of 10×). (a) Before applying a sinusoidal signal to the DEP chip; (b) applying an ac voltage of 20 V_{pp} with frequency of 1 MHz to the two Ag electrodes of DEP chip; (c) after switching off the applied signals; (d) re-applying the sinusoidal signals to the electrodes.

both the 5 μm- and 10 μm-diameter PS beads moved along a central streamline in the gap between the two electrodes, indicating that the 5 μm- and 10 μm-diameter PS beads exhibited n-DEP response in the applied frequency range. But the alignment positions of these two kinds of PS beads were in the center of the gap between two electrodes, rather than at the vicinity of the bottom electrode (as observed in figures 5(b) and (d)). It could be due to the different particle sizes and weights leading to the different polarization forces applied to the particles. The 5 μm-diameter PS beads were aligned and attached to the 10 μm-diameter PS beads. This may be due to a non-uniform electrical field generating a polarization region on the surface of the 10 μm-diameter PS beads with a larger surface area, which then attracts the smaller 5 μm-diameter beads to their surfaces.

The above DEP experimental results prove the feasibility of the fabricated DEP microfluidic chip with Ag electrodes for trapping microparticles with different sizes and from a mixture suspension. It is noted that the PS beads could also assemble on the Ag electrode surface due to a p-DEP force

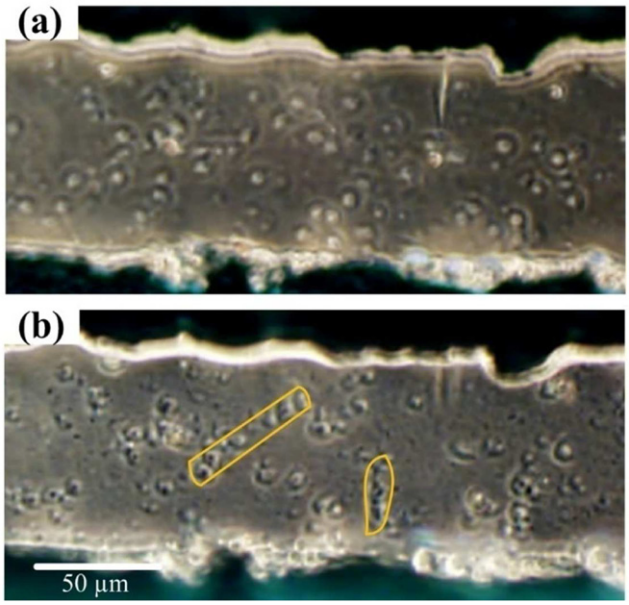

Figure 7. Microscopic images of a cell culture solution with cardiac fibroblasts of density of 10^6 cells ml^{-1} in the microchannel of a fabricated PMMA-based DEP microfluidic chip (magnification of 20×). (a) Before applying a sinusoidal signal to the DEP chip; (b) applying an ac voltage of 20 *V*pp with frequency of 1 MHz to the two Ag electrodes of DEP chip for 5 min.

in our experiment. But this could not be observed under the inverted microscope due to the non-transparent Ag electrodes used in this case. In addition, the alignment of PS beads can be used to quantify the DEP force applied to the beads by assessing the light intensity change on the electrode before and after applying the signal to the DEP chip [37].

3.4. Trapping of biological cells using the fabricated DEP microfluidic chip

To prove the feasibility of our DEP microfluidic chip for trapping biological cells, we selected cardiac fibroblasts as the target cell for the DEP experiment due to its approximately spherical shape and average cell diameter being close to 10 μm which is the average size of the day 2 cultured fibroblasts [38]. Before the DEP experiment, the cell viability and cell count were tested to ensure that the cells were alive. A cell density of 10^6 cells ml^{-1} in a suspension PBS medium with conductivity of 15.0×10^{-3} S m^{-1} was used in the following DEP experiments. As shown in figure 7(a), after injecting the PBS medium containing a suspension of cardiac fibroblasts to the DEP microfluidic chip, the cells distributed randomly in the microchannel of the DEP chip. After applying an ac voltage of 20 V_{pp} with frequency of 1 MHz to the Ag electrodes, some of fibroblasts moved to assemble and aligned in a line-shape (figure 7(b)), proving the feasibility of our DEP microfluidic chip to trap real cell samples. The alignment of the fibroblasts is not as obvious as of the PS beads observed above (figures 5–6), which could be due to the less conductive cell culture medium and the sticking of the adhesive fibroblast cells to the platform. As shown in figure 7, the orthogonal chain of fibroblasts happened at the edge of electrode when voltage

was supplied. The alignment of fibroblasts showed that of the gradient instantaneously produced on that particular surfaces; at right angles between the two electrodes.

Moreover, the effect of the competition between the DEP force and the gravity force on the particle trapping during the DEP experiment was also considered in our study [14]. Compared to the 3 μm- and 5 μm-diameter PS beads, the setting speed of the larger microparticles, such as 10 μm-diameter PS beads and cardiac fibroblasts, to the microchannel bottom of the DEP chip was fast due to their larger densities. Therefore, we used a 20 V_{pp} ac potential to generate a stronger DEP force in our experiment. In addition, according to previous studies [23], when the distance between the particle and the electrode surface is larger than 30 μm, the DEP force could be too weak to affect the particles. However, even when the PS beads were over 100 μm away from the electrode surface (figures 5(b) and 6(b)), the phenomenon of the particle trapping and alignment could still be observed. This might be due to the semi-three dimensional structure of our screen-printed Ag electrodes [32], which enhances the formation of the DEP field in the electrode gap and causes the particle polarization.

4. Conclusions

In summary, a facile and low cost screen-printing technique was developed and applied to fabricate silver electrodes on both solid/soft and transparent/non-transparent DEP substrates, including PMMA, PET and paper. And the fabricated DEP microfluidic chips on PMMA substrate was successfully used to trap polystyrene microparticles with different diameters, and the cardiac fibroblasts in sample solutions, proving the feasibility of the fabricated DEP microfluidic chip for both microparticles and biological cell trapping. The capability to fabricate DEP electrodes on different types of substrate could extend the potential application of DEP microfluidic devices, such as in the fields of point-of-care medicine, and clinical diagnosis. However, the size and the surface homogeneity of the electrodes fabricated by our method are still higher and coarser (respectively) than those made by the traditional DEP electrode fabrication techniques, such as electrochemical etching and metal deposition, due to the work principle and the spatial resolution limitation of the screen printing technique. Development of a screening mask with smaller size and higher resolution could contribute to improving the resolution of the screen-printing technique, therefore potentially extending the future application of screen-printing techniques for fabrication of DEP microfluidic chips.

Acknowledgments

This work was financially supported by the Key (Key grant) Project of Chinese Ministry of Education (313045), the Fundamental Research Funds for the Central Universities of China, the National Natural Science Foundation of China (21105079), the International Science & Technology Cooperation Program of China (2013DFG02930), the National Key Scientific Apparatus Development of Special Item (2013YQ190467), the Science and Technology Research and Development Program supported by Shaanxi Province of China (2012K08-18), Scientific Research Foundation for the Returned Overseas Chinese Scholars by the State Education Ministry of China, University Malaya High Impact Research Grant (UM.C/HIR/MOHE/ENG/44) from the Ministry of Education Malaysia and Postgraduate Research Grant (PPP) University Malaya (PV 102/2012A). In this paper, Wei Hong Wee accomplished the experiments and analysis, and prepared the draft manuscript. Zedong Li and Jie Hu assisted the experiments and data analysis. Fei Li and Nahrizul Adib Kadri did the experimental data analysis and proofed the manuscript. Belinda Pingguan-Murphy and Feng Xu secured the financial support for conducting the research, provided alternative insights on the analysis, and proofed the manuscript. All the authors participated in amending the manuscript.

Conflicts of interest

The authors declare no conflict of interest.

References

[1] VanDelinder V and Groisman A 2007 Perfusion in microfluidic cross-flow: separation of white blood cells from whole blood and exchange of medium in a continuous flow *Anal. Chem.* **79** 2023–30
[2] Koklu M *et al* 2010 Negative dielectrophoretic capture of bacterial spores in food matrices *Biomicrofluidics* **4** 15
[3] Antia M, Herricks T and Rathod P K 2007 Microfluidic modeling of cell–cell interactions in malaria pathogenesis *Plos Pathog.* **3** 939–48
[4] Dash S and Mohanty S 2014 Dielectrophoretic separation of micron and submicron particles: a review *Electrophoresis* **35** 2656–72
[5] Temiz Y, Skorucak J and Delamarche E 2014 Capillary-driven microfluidic chips with evaporation-induced flow control and dielectrophoretic microbead trapping *J. Micro/Nanolithogr. MEMS, MOEMS* **13** 033018
[6] Gossett D *et al* 2010 Label-free cell separation and sorting in microfluidic systems *Anal. Bioanal. Chem.* **397** 3249–67
[7] Labeed F H *et al* 2003 Assessment of multidrug resistance reversal using dielectrophoresis and flow cytometry *Biophys. J.* **85** 2028–34
[8] Nam J *et al* 2013 Magnetic separation of malaria-infected red blood cells in various developmental stages *Anal. Chem.* **85** 7316–23
[9] Čemažar J, Miklavčič D and Kotnik T 2013 Microfluidic devices for manipulation, modification and characterization of biological cells in electric fields–a review *Inf. Midem J. Microelectron. Electron. Compon. Mater.* **43** 143–61
[10] Whitesides G M 2006 The origins and the future of microfluidics *Nature* **442** 368–73
[11] Dou M W *et al* 2014 A versatile PDMS/paper hybrid microfluidic platform for sensitive infectious disease diagnosis *Anal. Chem.* **86** 7978–86
[12] Gupta V *et al* 2012 ApoStream™, a new dielectrophoretic device for antibody independent isolation and recovery of viable cancer cells from blood *Biomicrofluidics* **6** 024133

[13] Chiou P Y, Ohta A T and Wu M C 2005 Massively parallel manipulation of single cells and microparticles using optical images *Nature* **436** 3
[14] Samiei E, Rezaei Nejad H and Hoorfar M 2015 A dielectrophoretic-gravity driven particle focusing technique for digital microfluidic systems *Appl. Phys. Lett.* **106** 204101
[15] Chiou P Y, Zehao C and Ming W C 2003 A novel optoelectronic tweezer using light induced dielectrophoresis *Int. Conf. on Optical MEMS, 2003 IEEE/LEOS* p 2
[16] Ding X *et al* 2014 Cell separation using tilted-angle standing surface acoustic waves *Proc. Natl Acad. Sci.* **111** 12992–7
[17] Kirby D *et al* 2012 Centrifugo-magnetophoretic particle separation *Microfluid. Nanofluidics* **13** 899–908
[18] Prince M *et al* 2007 The development of a novel Bio-MEMS filtration chip for the separation of specific cells in fluid suspension *Proc. Inst. Mech. Eng. H: J. Eng. Med.* **221** 113–28
[19] Sebastian A, Buckle A M and Markx G H 2007 Tissue engineering with electric fields: immobilization of mammalian cells in multilayer aggregates using dielectrophoresis *Biotechnol. Bioeng.* **98** 694–700
[20] Voldman J 2006 Electrical forces for microscale cells manipulation *Annu. Rev. Biomed. Eng.* **8** 32
[21] Wang M W 2009 Using dielectrophoresis to trap nanobead/stem cell compounds in continuous flow *J. Electrochem. Soc.* **156** G97–102
[22] Cetin B, Özer M B and Solmaz M E 2014 Microfluidic bio-particle manipulation for biotechnology *Biochem. Eng. J.* **92** 63–82
[23] Martinez-Duarte R 2012 Microfabrication technologies in dielectrophoresis applications-a review *Electrophoresis* **33** 3110–32
[24] Muck A *et al* 2004 Fabrication of poly(methyl methacrylate) microfluidic chips by atmospheric molding *Anal. Chem.* **76** 2290–7
[25] Harrison D J *et al* 1992 Capillary electrophoresis and sample injection systems integrated on a planar glass chip *Anal. Chem.* **64** 1926–32
[26] McDonald J C and Whitesides G M 2002 Poly (dimethylsiloxane) as a material for fabricating microfluidic devices *Acc. Chem. Res.* **35** 491–9
[27] Martinez A W *et al* 2009 Diagnostics for the developing world: microfluidic paper-based analytical devices *Anal. Chem.* **82** 3–10
[28] Martinez A W, Phillips S T and Whitesides G M 2008 3D microfluidic devices fabricated in layered paper and tape *Proc. Natl Acad. Sci*. **105** 19606–611
[29] Sackmann E K, Fulton A L and Beebe D J 2014 The present and future role of microfluidics in biomedical research *Nature* **507** 181–9
[30] Nge P N, Rogers C I and Woolley A T 2013 Advances in microfluidic materials, functions, integration, and applications *Chem. Rev.* **113** 2550–83
[31] Gallo-Villanueva R C *et al* 2009 DNA manipulation by means of insulator-based dielectrophoresis employing direct current electric fields *Electrophoresis* **30** 4195–205
[32] Zhu H *et al* 2015 Screen-printed microfluidic dielectrophoresis chip for cell separation *Biosens. Bioelectron.* **63** 371–8
[33] Khoshmanesh K *et al* 2011 Dielectrophoretic platforms for bio-microfluidic systems *Biosens. Bioelectron.* **26** 1800–14
[34] Ruwhof C *et al* 2000 Cyclic stretch induces the release of growth promoting factors from cultured neonatal cardiomyocytes and cardiac fibroblasts *Mol. Cell. Biochem.* **208** 89–98
[35] Lin Y-Y, Welch E R and Fair R B 2012 Low voltage picoliter droplet manipulation utilizing electrowetting-on-dielectric platforms *Sensors Actuators B* **173** 338–45
[36] Gagnon Z R 2011 Cellular dielectrophoresis: applications to the characterization, manipulation, separation and patterning of cells *Electrophoresis* **32** 2466–87
[37] Kadri N A, Razak M A A and Ibrahim F 2012 Near real-time electrochemical analysis of carcinogenic cell lines using planar microelectrodes *Int. J. Electrochem. Sci.* **7** 5633–42
[38] Freitas R A 1999 *Nanomedicine, Volume I: Basic Capabilities* (Georgetown, TX: Landes Bioscience)